ChemComm

Accepted Manuscript

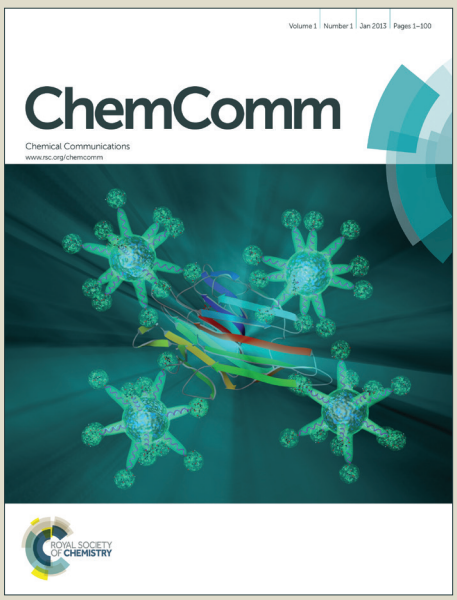

ROYAL SOCIETY OF CHEMISTRY

www.rsc.org/chemcomm

Journal Name

COMMUNICATION

Novel spiro-based hole transporting materials for efficient perovskite solar cells†

Received 00th January 20xx,
Accepted 00th January 20xx

DOI: 10.1039/x0xx00000x

www.rsc.org/

Ming-Hsien Li,‡[a] Che-Wei Hsu,‡[b] Po-Shen Shen,[a] Hsin-Min Cheng,[a] Yun Chi,[b*] Peter Chen,[a,c,d*] and Tzung-Fang Guo[a,c,d]

Three spiro-acridine-fluorene based hole transporting material (HTMs), namely: CW3, CW4 and CW5, are employed in fabrication of organic-inorganic hybrid perovskite solar cells. The corresponding mesoscopic $TiO_2/CH_3NH_3PbI_3$/HTM devices are investigated and compared with that made with commercial spiro-OMeTAD. The best conversion efficiency of 16.56% is achieved for CW4 in the presence of tBp and Li-TFSI as additives and without cobalt dopant. Performances of CW4 are further examined in terms of conductivity, mobility, morphology, and stability to show its potential as an alternative HTM.

Solid state organic-inorganic hybrid lead halide perovskite solar cells (PSCs) have been extensively studied and achieved power conversion efficiency (PCE) over 19%.[1-3] Superior characteristics such as ambipolar transport with long carrier diffusion length, small exciton binding energy, and broad light harvesting capability in visible region, have contributed to the remarkable performances of PSCs. Organic hole transport material (HTM) played an important role as selective contact for charge separation and extraction. Spiro-OMeTAD is the material commonly employed as the HTM for highly efficient solid-state dye-sensitized solar cell (ss-DSCs) and PSCs. Recently, many HTMs have been incorporated with perovskite with impressive solar energy conversion efficiency.[1, 3-8] Basically, the p-type contact materials for perovskite solar cell can be categorized according to their constituents, e.g. inorganic HTMs, polymeric HTMs and small molecular HTMs. Generally speaking, PSCs employed inorganic HTMs (i.e, NiO, CuI, CuSCN, and graphene oxide) have attracted much attention due to their higher mobility, high transparency in the visible region and good chemical stability.[4, 9-11] Moreover, organic HTMs are low-cost alternatives capable for low-temperature device processing. They are advantageous in providing diversified physical and optical properties to match the band gaps of various perovskites by modifying their structures. Thirdly, PSCs made with polymeric HTMs, such as oligothiophene,[12, 13] polyTPD,[14, 15] PDPPDBTE,[16] PCPDTBT,[17] PCDTBT,[17] PTAA,[17, 18] and P3HT,[17, 19, 20] have shown decent PCE. In contrast to polymeric HTMs with good stability and processibility, small molecular HTMs are easy to purify and suitable for forming crystalline thin films. Various small-molecule HTMs, such as arylamine functionalized pyrenes,[21] functional thiophene and bithiophenes,[6, 22] perylene,[23] BuPyIm-TFSI,[24] 3,4-ethylenedioxythiophene,[25, 26] triphenylamine,[27] triarylamine,[28] 2TPA-n-DP (n = 1-4),[29, 30] carbazole,[5] DATPA,[31] tetrathiafulvalene,[32] star-shaped triphenylamine,[33] spiro-OMeTAD,[7] and TPB based HTMs,[34] have been developed to show decent efficiencies between 11-16%. Encouraged by these discoveries, we developed a series of new HTMs with spiro-arranged acridine and fluorene moieties which can be readily prepared using large-scaled reaction and in high yield versus the widely used spiro-OMeTAD.

From the view point of structural design, di(p-methoxyphenyl)amine moiety of spiro-OMeTAD provides the higher lying HOMO for hole transport. The spiro-architecture ensured good thermal stability with increased steric interaction that prevents it from crystallization, which is advantageous for the infiltration into mesoscopic network structure. However, difficulty in purification and higher costs for production limited its potential for applications in low-cost solar cells. In this work, we report the novel alternative HTMs, namely CW3, CW4, and CW5, among which PSCs incorporated with CW4 achieve an efficiency of 14.81%. Synthesis of CW3, CW4, and CW5 are outlined in Scheme 1. Firstly, 4,4'-dimethoxydiphenylamine was treated with 2,7-dibromo-9H-fluoren-9-one using Buchwald-Hartwig coupling to afford the amine-substituted fluorenone in 85% yield. This fluorenone intermediate was next treated with a lithium derivative of functional triphenylamine, which was *in-situ* generated by addition of n-BuLi to the corresponding p-substituted 2-bromotriphenylamine.[35] Without further purification, the obtained alcohols were converted to the spiro-acridine-fluorene compounds

[a] *Department of Photonics, National Cheng Kung University, Tainan, Taiwan 701. E-mail: petercyc@mail.ncku.edu.tw*
[b] *Department of Chemistry, National Tsing Hua University, Hsinchu, Taiwan 300. E-mail: ychi@mx.nthu.edu.tw*
[c] *Research Center for Energy Technology and Strategy (RCETS), National Cheng Kung University, Tainan, Taiwan 701.*
[d] *Advanced Optoelectronic Technology Center (AOTC), National Cheng Kung University, Tainan, Taiwan 701.*

† Electronic Supplementary Information (ESI) available: Experiment, synthesis of HTMs, device fabrication, and characterization. Additional tables of performance of CW4-based perovskite solar cells with cobalt dopant. See DOI: 10.1039/x0xx00000x

‡ These authors contributed equally to this work.

CW3 – CW5 via a Friedel-Crafts intramolecular ring-closure reaction in high yield (> 60%). Among all compounds CW3 – CW5 synthesized, half of the structure possesses the key feature of spiro-OMeTAD to maintain the suitable HOMO energy level (i.e. -4.9 V) for hole transport, while the other half contains the functional acridine unit, for which the HOMO energy level should be slightly different, due to the distinctive molecular structure. Therefore, these compounds should possess several occupied molecular orbitals with minor differences in energy, which may be advantageous for efficient hole transport. Their high rigidity is also evident by the higher thermal decomposition temperatures (T_d, corresponding to 5% weight loss in the TG analysis) of 234 - 254°C and glass-transition temperatures (T_g) of 127 - 148°C. The lower molecular weights also ensure better pore filling ability versus spiro-OMeTAD under typical conditions. Electrochemical and thermal characteristics of spiro-OMeTAD, CW3, CW4, and CW5 are summarized in Table 1.

The device architecture shown in Figure 1(a) is based on the configuration of n-i-p mesoscopic heterojunction perovskite solar cell which is composed of FTO/compact (cp) TiO_2/mesoporous (mp) TiO_2/$CH_3NH_3PbI_3$/HTM/Au. A dense cp-TiO_2 blocking layer is first deposited on the FTO substrate by spray pyrolysis, while a mesoporous n-type mp-TiO_2 layer is formed by spin-coating of a diluted TiO_2 paste. The light harvesting $CH_3NH_3PbI_3$ layer was then applied to the porous network using solvent engineering reported by Seok to form a uniform and densely packed perovskite layer.[36] Experimentally, perovskite solution is prepared by dissolving 50 wt.% of $CH_3NH_3PbI_3$ in the mixed DMSO/GBL. The HTM is applied to the top of $CH_3NH_3PbI_3$ layer by spin-coating. Finally, an Au counter electrode is deposited by thermal evaporation. Figure 1(b) shows the cross-sectional SEM image of fabricated mesoporous perovskite solar cells that employ spiro-OMeTAD as HTM. Notably, thickness of capping layer of perovskite film is estimated to be ~400 nm, which allowed saturated light absorption and IPCE in the red-light range (see Fig. 2(b))

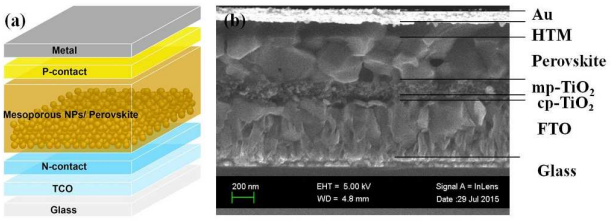

Fig. 1 (a) Device architecture and (b) cross-sectional SEM image of device employed sprio-OMeTAD.

It is well known that the solar cell performance can be improved significantly when 4-tert-butylpyridine (tBp) and lithium bis(trifluoromethylsulfonyl)imide (Li-TFSI) are added to the spiro-OMeTAD layer. Furthermore, certain cobalt or iridium metal complexes can be added as chemical dopant for improving the device performance.[21, 37, 38] Thus, many studied PSCs were doped with tBp and Li-TFSI[6, 13, 16, 17, 21, 30, 33, 34, 38] or with tBp, Li-TFSI and cobalt dopant FK102.[39] Their conductivity and mobility were

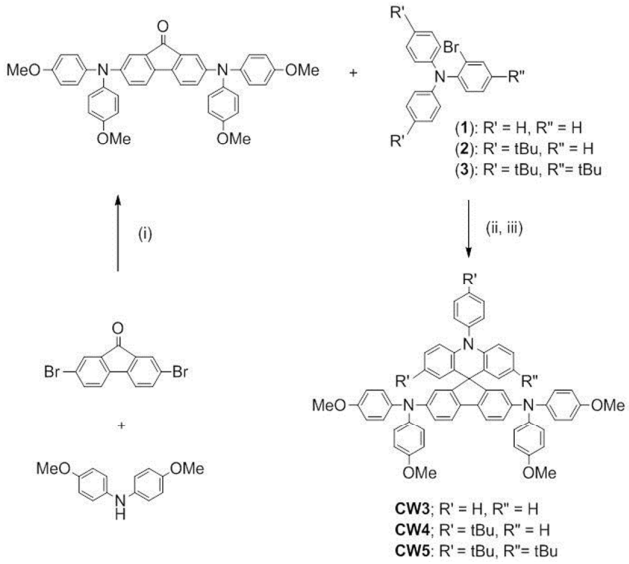

Scheme 1. Synthetic procedures for CW3, CW4, and CW5; experimental conditions: (i) $Pd(dba)_2$, $P(tBu)_3$, NaOtBu, toluene, reflux, (ii) n-BuLi, -78 °C, (iii) HCl, AcOH, reflux.

measured with a flat junction configuration where the spin-coated HTM is sandwiched between the FTO substrate and thermally evaporated gold electrode. Hole conductivity of CW3, CW4, and CW5 are measured to be 5.92, 3.54 and 3.09 x 10^{-6} S-cm^{-1}, respectively. By fitting the J-V curves with Mott-Gurney equation, hole mobility of HTMs are estimated to be 1.2, 0.58 and 0.87 x 10^{-4} $cm^2V^{-1}S^{-1}$, respectively. Although the change in electrical properties is minimal, its variation can still be correlated to the associated molecular size and observed T_g. Figure 2(a) shows current density-voltage (J-V) curves of the solar cells using spiro-OMeTAD, CW3, CW4, and CW5 with tBp and Li-TFSI as additives, while their numeric data are summarized in Table 1. The CW4-based device gives a J_{SC} of 21.75 mA/cm^2, V_{OC} of 1050 mV, and FF of 72%, with a PCE of 16.56% under AM 1.5 G illumination. Under similar fabrication condition, the CW3- and CW5-based PSCs show a J_{SC} of 15.83 and 15.17 mA/cm^2, V_{OC} of 1040 and 1060 mV, FF of 74% and 78%, and PCE of 12.33% and 12.62%, respectively. To check reproducibility on the performance for CW4-based device, the statistic histograms are performed as presented in Fig. S1. Eventually, CW4-based perovskite solar cell displays J_{SC} of 20.55±1.31 $mAcm^{-2}$, V_{OC} of 1046±17 mV, FF of 0.66±0.04, and PCE of 14.14±1.47. Stability of encapsulated (under ambient condition) PSC employed CW4 and spiro-OMeTAD are monitored as displayed in Fig. S2(a). The normalized PCE significantly decreases with an exposure time over 10 hr. The results might be attributed to the instability of $MAPbI_3$.[40] Furthermore, residual humility inside the sealed device would penetrate along the pinholes of HTM to damage the devices (as seen in Fig S3). The long-term stability of spiro-OMeTAD and CW4 is monitored with flat p-n junction configuration composed of FTO/cp-TiO_2/HTM/Au. Figure S2(b) and S2(c) present the evolution of their J-V curves under light soaking. Similar trend of J-V curves are observed before 174 hr as displayed in Fig. S2(d).

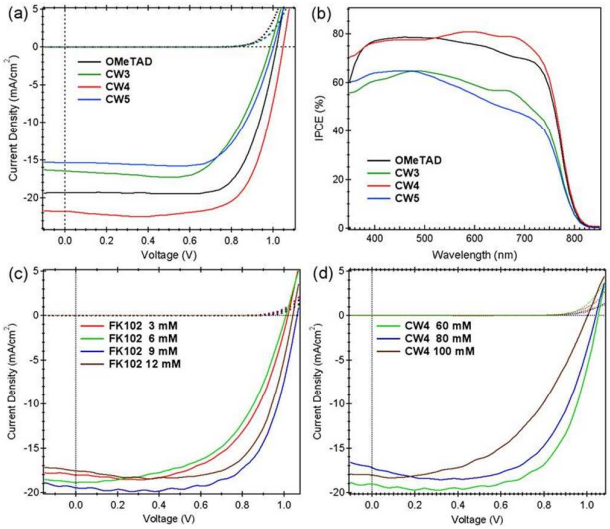

Fig. 2 (a) The J-V characteristics and (b) IPCE action spectra of the devices with various HTMs. (c) The J-V curves of devices with CW4 at different concentration of cobalt dopant (FK102) and (d) devices with different concentration of CW4 under constant FK102 doping.

PSCs employ CW4 present the highest J_{SC} and PCE, which is superior to that of reference device employing spiro-OMeTAD. The conductivity for all these HTMs appeared to be dependent on the hole hoping distances.[41] The CW3 has no alkyl substituents, so that the smallest intermolecular separation reduces the hole hoping barrier between the molecules. This is revealed in the conductivity measurement where the CW3 has the highest conductivity than the others. However, in the device application where the kinetic interfacial charge transfer has to be taken into account. The small molecular size of CW3 probably leads to an inferior morphological coverage over the perovskite layer, leading to inferior hole extraction and lower photocurrent. On the contrary, as the size of substituents is increased for CW4, the increased steric interaction may leads to a conformal coating on top of perovskite and resulted in a better photocurrent. As for CW5, the three bulky *t*-butyl substituents wrapping around the acridine fragment may restrain the inter-molecular carrier hopping, as shown in its lowest conductivity and, hence, the lowest current. The interplay between the steric interaction and morphological coverage is very complex and required further investigation to fully understand their impacts to the photovoltaic performances.

The photocurrent action spectra of four PSC devices are presented in Figure 2(b). Notably, CW4 device exhibits IPCE of ~80% which is superior to that displayed by spiro-OMeTAD. Surface morphology SEM images of spiro-OMeTAD and CW4 spin-coated on perovskite film are analyzed as shown in Figure S3. The results indicate that CW4 HTM layer displayed a uniform coverage over perovskite thin film. It is believed that better coverage of CW4 on the perovskite film is beneficial to the IPCE response. Addition of cobalt dopant FK-102 was also attempted for further optimization of devices. Figure 2(c) displays the J-V curves of devices with different doping concentration of FK102 in CW4, while the detailed performance parameters are summarized in Table S1. Surprisingly, these devices failed to show any improvement over the un-doped devices. This can be partially attributed to the extreme thin layer of HTM that has very limited influences on the charge transport despite of the increased conductivity. Another contribution is probably resulted from the lowered inherent electron mobility of TiO_2. Thus, unbalanced charge transport may result in higher recombination in the PSC with highly doped HTM.[42]

Generally speaking, HTM forms flat junction on the top of perovskite layer without infiltration into the mesoscopic cavity in PSCs. This situation is unlike to the ss-DSCs where the carrier would travel for a distance of ~2 μm in the mesoscopic TiO_2, so that the enhanced conductivity of doped HTM would have exhibited significant impact on the charge transport and especially the fill factor of device (FF).[39] Similar effect on the photovoltaic performance has been reported in recent literatures, although the mechanism was not yet clarified.[32, 43] Moreover, the PCE seems to be more sensitive to the HTM layer thickness, i.e. the conc. of HTM solution. This is revealed in the J-V curves and performance parameters of devices with a fixed conc. of FK102 at 9 mM and varied conc. of CW4, as shown in Figure 2(d) and Table S2, respectively. The results show that device utilizing 60 mM of CW4 presents the highest efficiency of 13.62% which is slightly lower than that of the best device without the added FK102 (e.g. 14.81 %). With progressively increasing the HTM concentration, the increased thickness of HTM results in the reduced carrier transport, versus the device prepared using the lowest conc. of 60 mM, at which the series resistance of HTM is at the minimal. Thus, the thickness of HTM above the perovskite layer is crucial for achieving descent efficiency.

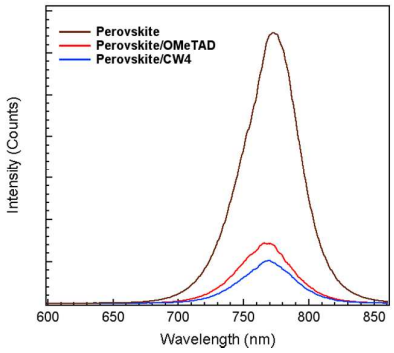

Fig. 3 Photoluminescence (PL) spectra of parent perovskite film, and spiro-OMeTAD and CW4 dopped thin film on quartz glass, all excited at 532 nm.

Steady-state photoluminescence (PL) measurement is applied to investigate the charge carrier recombination behavior in the bulk perovskite and between the perovskite/HTM interface, as shown in Figure 3. A considerable decrease in PL intensity was observed for the perovskite film doped with both spiro-OMeTAD and CW4. The enhanced quenching indicates effective charge extraction, which is in good agreement with the remarkable performance displayed by both HTMs.

In summary, spiro-arranged acridine and fluorene based HTMs were synthesized and applied in fabrication of $CH_3NH_3PbI_3$ based perovskite solar cells, among which the host CW4 showed the highest PCE of 16.56% in absence of cobalt dopant. The recorded

performance characteristic is comparable to that of the standard PSC fabricated using commercial spiro-OMeTAD under identical architecture (14.32%). Moreover, electronic properties, surface morphology and stability of CW4 are analyzed to present a compatible performance as compared to spiro-OMeTAD, These results show that, after optimization of structure, CW4 can be a promising and cost-effective HTM for perovskite solar cells.

Table 1. Characteristic parameters of spiro-OMeTAD, CW3, CW4, and CW5 and photovoltaic parameters for perovskite solar cells using these HTMs

HTM	HOMO (eV)	LUMO (eV)	Eg (eV)	Tg (°C)	Tm (°C)	Conductivity ($S\text{-}cm^{-1}$)	Mobility * ($cm^{2}\text{-}v^{-1}\text{-}s^{-1}$)	V_{OC} (mV)	J_{SC} ($mA\text{-}cm^{-2}$)	FF	PCE (%)
spiro-OMeTAD	-4.96	-1.98	2.98	125	248	$6.14x10^{-6}$	$2.0x10^{-4}$	1020	19.35	0.73	14.32
CW3	-4.92	-1.89	3.03	127	254	$5.92x10^{-6}$	$1.2x10^{-4}$	989	16.49	0.67	10.94
CW4	-4.92	-1.88	3.04	142	238	$3.54x10^{-6}$	$5.8x10^{-5}$	1050	21.75	0.72	16.56
CW5	-4.93	-1.89	3.04	148	234	$3.09x10^{-6}$	$8.7x10^{-5}$	1005	15.39	0.70	10.76

* Mobility of HTMs is estimated by the Mott-Gurney equation with the same dielectric constant of 3.

Notes and references

Y. C., P. C. and T.-F. G. acknowledge the funding from the Ministry of Science and Technology (MOST) of Taiwan under the grant-in-aids (103-2119-M-007-002), (103-2221-E-006-029-MY3), and (103-2119-M-006-020) respectively.

1. H. Zhou, Q. Chen, G. Li, S. Luo, T.-b. Song, H.-S. Duan, Z. Hong, J. You, Y. Liu and Y. Yang, *Science*, 2014, **345**, 542.
2. http://www.nrel.gov/ncpv/images/efficiency_chart.jpg.
3. C.-C. Chueh, C.-Z. Li and A. K. Y. Jen, *Energy Environ. Sci.*, 2015, **8**, 1160.
4. J. H. Kim, P.-W. Liang, S. T. Williams, N. Cho, C.-C. Chueh, M. S. Glaz, D. S. Ginger and A. K. Y. Jen, *Adv. Mater.*, 2015, **27**, 695.
5. S. D. Sung, M. S. Kang, I. T. Choi, H. M. Kim, H. Kim, M. Hong, H. K. Kim and W. I. Lee, *Chem. Commun.*, 2014, **50**, 14161.
6. H. Li, K. Fu, P. P. Boix, L. H. Wong, A. Hagfeldt, M. Grätzel, S. G. Mhaisalkar and A. C. Grimsdale, *ChemSusChem*, 2014, **7**, 3420.
7. N. J. Jeon, H. G. Lee, Y. C. Kim, J. Seo, J. H. Noh, J. Lee and S. I. Seok, *J. Am. Chem. Soc.*, 2014, **136**, 7837.
8. K. Wojciechowski, S. D. Stranks, A. Abate, G. Sadoughi, A. Sadhanala, N. Kopidakis, G. Rumbles, C.-Z. Li, R. H. Friend, A. K. Y. Jen and H. J. Snaith, *ACS Nano*, 2014, **8**, 12701.
9. K.-C. Wang, P.-S. Shen, M.-H. Li, S. Chen, M.-W. Lin, P. Chen and T.-F. Guo, *ACS Appl. Mater. Interfaces*, 2014, **6**, 11851.
10. M.-H. Li, P.-S. Shen, K.-C. Wang, T.-F. Guo and P. Chen, *J. Mater. Chem. A*, 2015, **3**, 9011.
11. Z. Wu, S. Bai, J. Xiang, Z. Yuan, Y. Yang, W. Cui, X. Gao, Z. Liu, Y. Jin and B. Sun, *Nanoscale*, 2014, **6**, 10505.
12. L. Zheng, Y.-H. Chung, Y. Ma, L. Zhang, L. Xiao, Z. Chen, S. Wang, B. Qu and Q. Gong, *Chem. Commun.*, 2014, **50**, 11196.
13. P. Qin, H. Kast, M. K. Nazeeruddin, S. M. Zakeeruddin, A. Mishra, P. Bauerle and M. Gratzel, *Energy Environ. Sci.*, 2014, **7**, 2981.
14. C. Roldan-Carmona, O. Malinkiewicz, A. Soriano, G. Minguez Espallargas, A. Garcia, P. Reinecke, T. Kroyer, M. I. Dar, M. K. Nazeeruddin and H. J. Bolink, *Energy Environ. Sci.*, 2014, **7**, 994.
15. O. Malinkiewicz, A. Yella, Y. H. Lee, G. M. Espallargas, M. Graetzel, M. K. Nazeeruddin and H. J. Bolink, *Nat. Photon.*, 2014, **8**, 128.
16. Y. S. Kwon, J. Lim, H.-J. Yun, Y.-H. Kim and T. Park, *Energy Environ. Sci.*, 2014, **7**, 1454.
17. J. H. Heo, S. H. Im, J. H. Noh, T. N. Mandal, C.-S. Lim, J. A. Chang, Y. H. Lee, H.-j. Kim, A. Sarkar, M. K. Nazeeruddin, M. Gratzel and S. I. Seok, *Nat. Photon.*, 2013, **7**, 486.
18. S. Ryu, J. H. Noh, N. J. Jeon, Y. Chan Kim, W. S. Yang, J. Seo and S. I. Seok, *Energy Environ. Sci.*, 2014, **7**, 2614.
19. M. Zhang, M. Lyu, H. Yu, J.-H. Yun, Q. Wang and L. Wang, *Chem. Eur. J.*, 2015, **21**, 434.
20. F. Di Giacomo, S. Razza, F. Matteocci, A. D'Epifanio, S. Licoccia, T. M. Brown and A. Di Carlo, *J. Power Sources*, 2014, **251**, 152.
21. N. J. Jeon, J. Lee, J. H. Noh, M. K. Nazeeruddin, M. Grätzel and S. I. Seok, *J. Am. Chem. Soc.*, 2013, **135**, 19087.
22. T. Krishnamoorthy, F. Kunwu, P. P. Boix, H. Li, T. M. Koh, W. L. Leong, S. Powar, A. Grimsdale, M. Gratzel, N. Mathews and S. G. Mhaisalkar, *J. Mater. Chem. A*, 2014, **2**, 6305.
23. A. Ishii, A. K. Jena and T. Miyasaka, *APL Mat.*, 2014, **2**, 091102.
24. H. Zhang, Y. Shi, F. Yan, L. Wang, K. Wang, Y. Xing, Q. Dong and T. Ma, *Chem. Commun.*, 2014, **50**, 5020.
25. H. Li, K. Fu, A. Hagfeldt, M. Grätzel, S. G. Mhaisalkar and A. C. Grimsdale, *Angew. Chem. Int. Ed.*, 2014, **53**, 4085.
26. A. Krishna, D. Sabba, H. Li, J. Yin, P. P. Boix, C. Soci, S. G. Mhaisalkar and A. C. Grimsdale, *Chem. Sci.*, 2014, **5**, 2702.
27. S. Lv, L. Han, J. Xiao, L. Zhu, J. Shi, H. Wei, Y. Xu, J. Dong, X. Xu, D. Li, S. Wang, Y. Luo, Q. Meng and X. Li, *Chem. Commun.*, 2014, **50**, 6931.
28. J. Xiao, L. Han, L. Zhu, S. Lv, J. Shi, H. Wei, Y. Xu, J. Dong, X. Xu, Y. Xiao, D. Li, S. Wang, Y. Luo, X. Li and Q. Meng, *RSC Adv.*, 2014, **4**, 32918.
29. J. Wang, S. Wang, X. Li, L. Zhu, Q. Meng, Y. Xiao and D. Li, *Chem. Commun.*, 2014, **50**, 5829.

30. L. Zhu, J. Xiao, J. Shi, J. Wang, S. Lv, Y. Xu, Y. Luo, Y. Xiao, S. Wang, Q. Meng, X. Li and D. Li, *Nano Res.*, 2014, DOI: 10.1007/s12274-014-0592-y, 1.
31. A. Abate, M. Planells, D. J. Hollman, V. Barthi, S. Chand, H. J. Snaith and N. Robertson, *Phys. Chem. Chem. Phys.*, 2015, **17**, 2335.
32. J. Liu, Y. Wu, C. Qin, X. Yang, T. Yasuda, A. Islam, K. Zhang, W. Peng, W. Chen and L. Han, *Energy Environ. Sci.*, 2014, **7**, 2963.
33. H. Choi, S. Park, S. Paek, P. Ekanayake, M. K. Nazeeruddin and J. Ko, *J. Mater. Chem. A*, 2014, **2**, 19136.
34. Y. Song, S. Lv, X. Liu, X. Li, S. Wang, H. Wei, D. Li, Y. Xiao and Q. Meng, *Chem. Commun.*, 2014, **50**, 15239.
35. K.-Y. Liao, C.-W. Hsu, Y. Chi, M.-K. Hsu, S.-W. Wu, C.-H. Chang, S.-H. Liu, G.-H. Lee, P.-T. Chou, Y. Hu and N. Robertson, *Inorg. Chem.*, 2015, **54**, 4029.
36. N. J. Jeon, J. H. Noh, Y. C. Kim, W. S. Yang, S. Ryu and S. I. Seok, *Nat. Mater.*, 2014, **13**, 897.
37. L. Badia, E. Mas-Marzá, R. S. Sánchez, E. M. Barea, J. Bisquert and I. Mora-Seró, *APL Mat.*, 2014, **2**, 081507.
38. J. H. Noh, N. J. Jeon, Y. C. Choi, M. K. Nazeeruddin, M. Gratzel and S. I. Seok, *J. Mater. Chem. A*, 2013, **1**, 11842.
39. J. Burschka, A. Dualeh, F. Kessler, E. Baranoff, N.-L. Cevey-Ha, C. Yi, M. K. Nazeeruddin and M. Grätzel, *J. Am. Chem. Soc.*, 2011, **133**, 18042.
40. T.-B. Song, Q. Chen, H. Zhou, C. Jiang, H.-H. Wang, Y. Yang, Y. Liu, J. You and Y. Yang, *Journal of Materials Chemistry A*, 2015, **3**, 9032.
41. S. T. Bromley, M. Mas-Torrent, P. Hadley and C. Rovira, *J. Am. Chem. Soc.*, 2004, **126**, 6544.
42. C. S. Ponseca, T. J. Savenije, M. Abdellah, K. Zheng, A. Yartsev, T. Pascher, T. Harlang, P. Chabera, T. Pullerits, A. Stepanov, J.-P. Wolf and V. Sundström, *J. Am. Chem. Soc.*, 2014, **136**, 5189.
43. P. Ganesan, K. Fu, P. Gao, I. Raabe, K. Schenk, R. Scopelliti, J. Luo, L. H. Wong, M. Gratzel and M. K. Nazeeruddin, *Energy Environ. Sci.*, 2015, DOI: 10.1039/C4EE03773A.